Outdoor-to-Indoor and Indoor-to-Indoor Propagation Path Loss Modeling Using Smart 3D Ray Tracing Algorithm at 28 GHz mmWave

Ubaid Ullah[1] · Usman Rauf Kamboh[1] · Ferdous Hossain[2] · Muhammad Danish[1]

Abstract

The goal of the article is to provide a radio propagation algorithm for an outdoor-to-indoor and indoor-to-indoor environment for 5G mmWave in a populated city. This work is done by simulating a smart 3D ray tracing algorithm in MATLAB. The research here is done by taking into account the 28 [GHz] operating frequency which is potential for 5G network. The received results are provided in form of path loss and received signal strength. The results obtained show that a moderate outdoor-to-indoor service can be provided at the above-mentioned frequency. Two indoor path loss models (WINNER II and ITU-R) are also compared here. The literature review provided here is sufficient enough to prove that there is still a huge gap between the conventional ray tracing methods. The proposed model here deals with radio propagations using speedy computations and efficient use of resources. The findings of this paper also include that the path loss is also dependent on the separation between transmitter and receiver, the structure of the building and number and type of the obstructions in the path of RF waves.

Keywords Femtocell · Macro-cell · 3D ray tracing · LoS · NLoS

1 Introduction

Wireless communication system is one of the growing systems nowadays. Each year the demanding data for mobile communications are growing. The number of subscribers is increasing exponentially while network providers are bound to provide cheap and reliable services due to market competition. The demand for large bandwidth is a huge impediment for wireless service providers in such a competitive environment. Nowadays femto base stations have been deployed in houses, offices, bus stations, airports, malls, educational institutes, hospitals, subways, etc., due to their high capacity, better coverage, low cost and high spectrum efficiency [1].

A typical path loss model comprises of three major components

1. Large-scale propagation losses

✉ Ubaid Ullah
  ubaid.ullah@tuf.edu.pk

1 School of Computational Science, The University of Faisalabad, Punjab 38000, Pakistan

2 Faculty of Engineering and Technology, Multimedia University, 75450 Melaka, Malaysia

2. Wall loss
3. Indoor path losses

The frequently used path loss models are COST231 [2], 3GPP [3], WINNER project [4] and ITU-R [5]. Regardless of the fact that each model is derived with different aspects, we have found that femtocells have discrepancies of 10 [dB] with 100 [m] of radius. The above-mentioned models were derived in consideration with only 1 [km] radius. In [2], the measurements were carried out at 0.9 [GHz] and 1.8 [GHz] derived the COST 231 model. However, many concerned approaches to the model were not successful in providing the desired results.

On the basis of previous studies [6–8], the propagation (path loss) models are divided into two main categories.

(a) site-specific propagation model
(b) statistical models.

For outdoor and indoor propagation cases, various statistical/empirical propagation models exist which rely on measurement data [9]. The current empirical models Walfisch–Ikegami model, Longley–Rice model, Okumura–Hata model, PCS extension to Hata model, Durkin's model, [6] have been
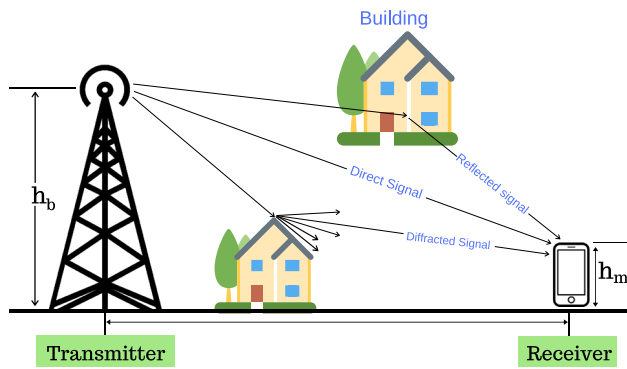
Fig. 1 Ray tracing technique [3]

used for outdoor case, and the existing empirical models for indoor cases are ITU, log-normal shadowing model, Ericsson multiple breakpoint model, indoor propagation model, log distance path loss model, attenuation factor model [10]. For sake of rendering (generating images or animations) in 3D computer graphics, ray-tracing methods have been utilized effectively; however, for making practical methods in radio propagation based on ray tracing, many years have gone into the study and experimentation to make estimations that can reflect the specific environment. The technique of RF ray tracing (RT) was adopted from computer graphics and is now widely used in wireless communications. The first idea of RF ray tracing using and algorithm was presented by Ikegami et al. [2]. The modern RT algorithms use virtual reality based waves and reality-based models and consider major paths. On the basis of rays handling, the modern algorithms are divided into three major groups of computations. Brute force ray tracing [11] can be used in complex environments, but it needs reception tests. In this proposed model, the environment is complex and unsymmetrical; therefore, we chose Brute force ray tracing technique and improved its reception tests, as well as its computational time. An overview of a ray-tracing technique for predicting radio propagation is shown in Fig. 1 [12].

Recent studies show that using omnidirectional path loss models by using a directional antenna can reveal accurate distance and frequency path loss modeling for indoor at 28 [GHz] [13]. The same is done for urban scenarios as well [14]. Probabilistic omnidirectional propagation model at frequencies 28 [GHz] and 73 [GHz] for outdoor environment [15] estimates coverage, outage and interference. Sulyman et al. [16] presented an industrial standard path loss model that can have capacity gains 20 times higher than LTE. Propagation characteristics at 11, 16, 28 and 38 [GHz] mmWave band were conducted using space-altering generalized expectation to investigate the wavefront, non-stationarity property, cluster birth–death [17,18]. The work reported here conducts the simulations on mmWave of frequency band 28 [GHz] to model a propagation algorithm that can estimate path loss for
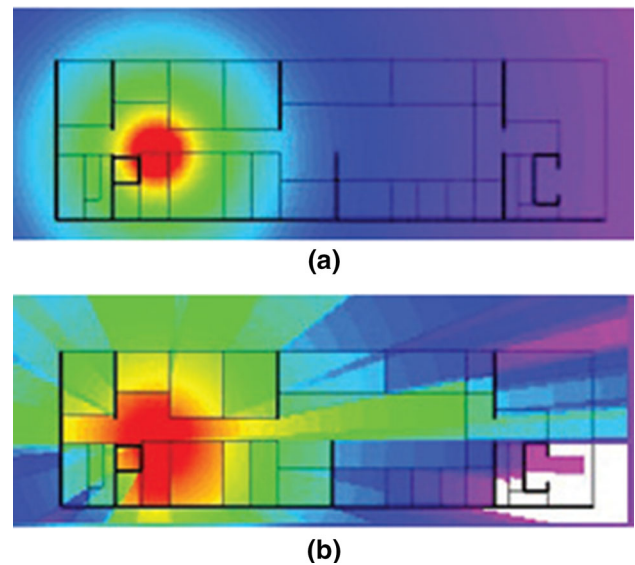

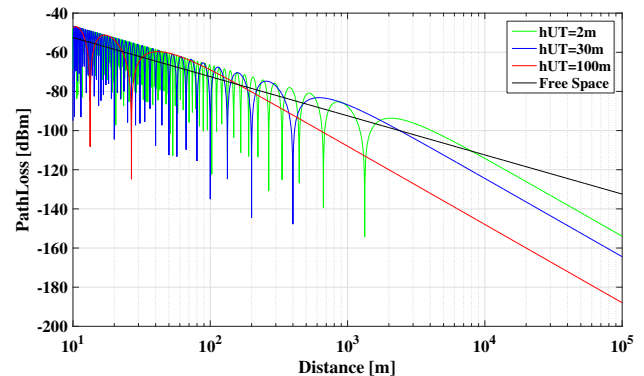Fig. 2 Examples of previous work done [3]

Fig. 3 A demonstration of two-ray model

an urban scenario for both outdoor as well as indoor environment.

The article is structured as follows. Section 2 defines the measurement and the under-discussion scenario, Sect. 3 discusses the empirical approach for path loss estimations, Sect. 4 explains the ray tracing concerned to the under consideration scenario, and Sect. 5 is concerned with the results. In Sect. 6, conclusion and future work are discussed (Figs. 2, 3).

2 Concerned Scenario

In this section, a macro-femto network consisting of macro base station (MBS) installed with group of femto base stations has been contemplated. The two discussed base stations (FBSs and MBS) are supposed to be operating using same licensed frequencies bands and using same technology (OFDMA). Considering that MBS is ensuring the com-

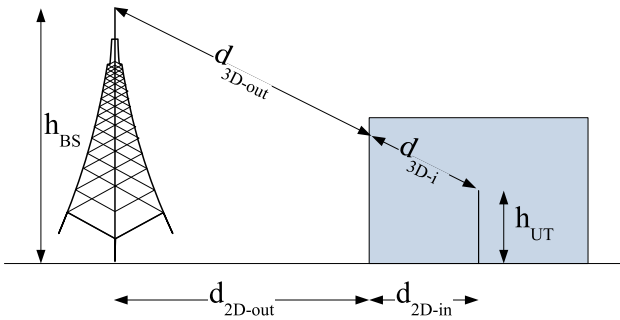**Fig. 4** Aerial view of the concerned scenario

Fig. 5 3D distance explanation [21]

plete coverage, we deploy femtocells to ensure the increased throughput and divide the traffic from macro-cell. The base stations (BS) were fixed, and the mobile station (MS) was moving outdoors (UMa case) or indoors (O2I case).

Figure 4 illustrates the aerial view of the concerned campaign for urban macro-cell. The macro BS shown in Fig. 4 (with red circle) is set at a height of 30 [m]. The height and distance from BS to MS vary as the user moves within the building or outside the building. The experimental location lies within latitudes 31.423817″ N and longitudes 73.077476″ E in the northwestern part of Faisalabad city in Punjab Province of Pakistan. The gross floor area of the building is 8715 [m^2] with the height of 50.4 [m]. The building comprises of 15 floors including 2 floors in the basement with 13 to 15 users on each floor. The site has high-rise building on both sides of the road with a road width of 10 [m].

Our research question is to find out the path loss which will analyze the effect of macro-cell in outdoor environment and indoor environment, femtocell in an indoor environment. Femtocell is used in indoor surroundings or buildings. The main problem is to check and analyze the performance of femtocell as compared to macro-cell and indoor environment losses due to obstacle within the building.

3 Empirical Path Loss Modeling

The major components of empirical path loss modeling are (a) the building database and (b) electromagnetic parameter database [19]. The electromagnetic waves reflect when they strike an electrical object having larger dimensions than wavelength [6]. The electromagnetic parameters include the permittivity of transmission coefficients, concrete walls, conductivity, ceiling, floor, polarization information and reflection coefficients.

3.1 Empirical Path Loss Modeling for O2I

The basic path loss for (line of sight) LoS condition is modeled here as: [20]

$$PL_T = PL_b + PL_{tw} + PL_{in} + N(0, \sigma_P^2) + N(0, \sigma_{SF}^2) \quad (1)$$

where PL_b is the typical path loss, PL_{tw} is the building penetration losses through the outer wall of the building and PL_{in} is the in-building path loss. σ_P^2 is the standard deviation for the penetration losses of the building, and σ_{SF}^2 is standard deviation for shadow fading (Fig. 5).

If a user is dropped in a network, the very first step is to find whether situation is LoS or NLoS. [20]

$$PL_b = PL_{3D_{UMa}}(d_{3D_{out}} + d_{3D_{in}}) \quad (2)$$

where $PL_{3D_{UMa}}$ is the path loss for macro base station, $d_{3D_{out}}$ is the 3-dimensional distance outside the building and $d_{3D_{in}}$ is the indoor three-dimensional distance [20].

$$PL_{UMa\text{-}LOS} = 32.2 + 40 * \log_{10}(d_{3D}) + 20 * \log_{10}(f_c) - \\ 10 * \log_{10}(d_{BP'})^2 + (h_{BS} - h_{UT})^2) \quad (3)$$

in Eq. (3) f_c represents carrier frequency, h_{BS} represents base station height, h_{UT} is the user terminal height and d'_{BP} represents break-point distance, modeled here as [20]

$$d_{BP'} = \frac{4h'_{BS}h'_{UT}f_c}{c} \quad (4)$$

h'_{BS} and h'_{UT} are the effective antenna heights for BS and UE. c is the speed of light. d_{3D} is the 3-dimensional (3D) distance from transmitter to receiver and is given by [20] as

$$d_{3D\text{-}out} + d_{3D\text{-}in} = d_{3D} \\ = \sqrt{(d_{2D_{out}} + d_{2D_{in}})^2 + (h_{BS} - h_{UT})^2} \quad (5)$$

$d_{2D_{out}}$ is the two-dimensional distance outside the building and $d_{2D_{in}}$ is the indoor two-dimensional distance. The building penetration loss modeled here is taken into account from

Table 1 Path loss through building

	Path loss through external wall PL_{tw}
Traditional infrastructure	$5 - 10 * log_{10}(0.3 * 10^{-\frac{S_{gl}}{10}} + 0.7 * 10^{-\frac{Conc}{10}})$
Modern infrastructure	$5 - 10log_{10}(0.7 * 10^{-\frac{IRR_{gl}}{10}} + 0.3 * 10^{-\frac{Conc}{10}})$
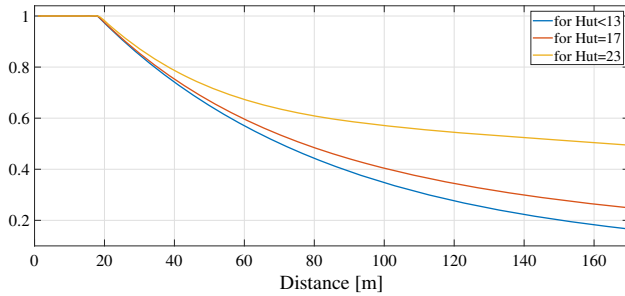
Fig. 6 Macro loss probability
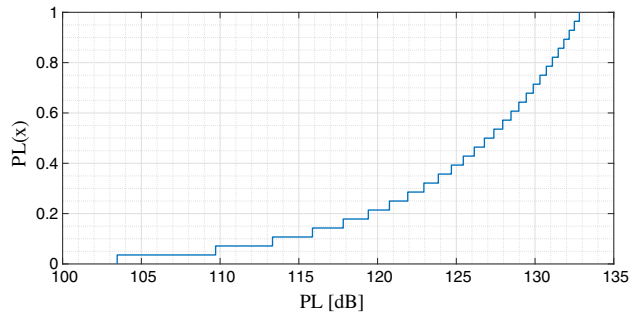
Fig. 7 Empirical CDF for macro BS

[3]

$$L_{mat} = a_{mat_i} + b_{mat_i}.f \qquad (6)$$

In Eq. (6) a_{mat_i} and b_{mat_i} are constants. The value of a_{mat_i} and b_{mat_i} changes with the type of material used in buildings. For example, for wood $a_{mat_i} = 4.85$ and $b_{mat_i} = 0.12$, for concrete $a_{mat_i} = 5$ and $b_{mat_i} = 4$.

The building cannot be built with single material. Therefore, a composition of penetration losses is modeled. Table 1 illustrates the two main types of penetration losses for modern and traditional infrastructures (Figs. 6, 7).

In Table 1, S_{gl} is the path loss through single glass, $Conc$ is the path loss through concrete and IRR_{gl} is the path loss through infrared reflected glass. The in-building loss is given by [3]

$$PL_{in} = \alpha d_{2_{Din}} \qquad (7)$$

where α is the in-building constant and its value depends on the type of material used in building. For the concerned, the value of α is 0.5.
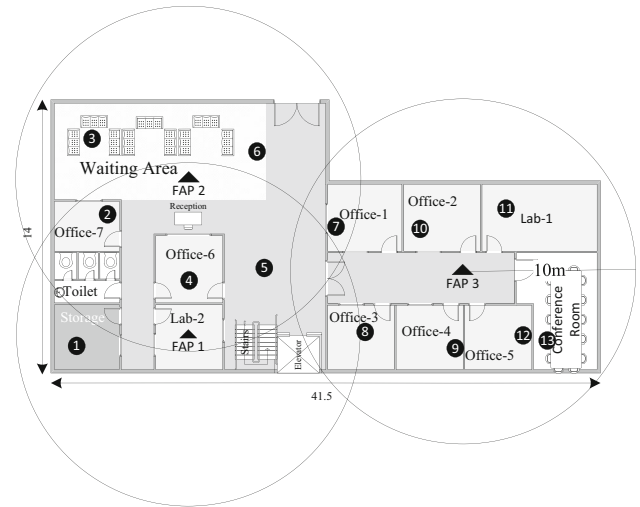
Fig. 8 Femto deployment on the basis of radius covered

Table 2 Distance between FAPs and FUTs

FUT	FAP1	FAP2	FAP3
1	6	11.7	23
2	8.3	5.1	21.1
3	12.7	6.1	23.1
4	3.1	5.9	16.1
5	5.9	6.8	11.7
6	11.4	4.3	14
7	10.6	9	8
8	10.3	13.6	6.8
9	15.6	18.4	4.4
10	14.8	13.8	3.6
11	19.9	18.6	4.4
12	19.4	21.5	5
13	20.9	22.9	6.2

3.2 Empirical Path Loss for Femtocell

The femtocells, which are specific to 3GPP standard, are also called as Home NodeB. Along with femtocells, all other equipments required for the integration of present network are illustrated with different deployment techniques. Due to the limitation of radio spectrum, new and effective solutions are required. In densely populated urban areas, variety of cell sizes (nano, pico, femto, micro, macro) are used for the betterment of user capacity. The femtocells support approx. all the main cellular standardized protocols, i.e., WCDMA,
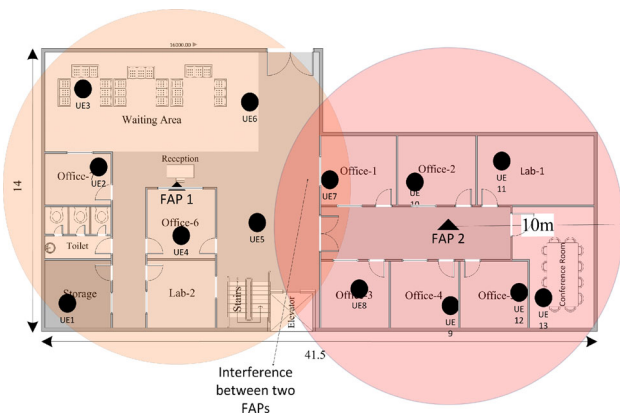
Fig. 9 Intelligent femto deployment on the basis of coverage area

Table 3 Simulation parameters

| Parameter	Symbol	Value
Initial femtocell radius	$Rfini$	10 m
Initial macro-cell radius	$Rmini$	577 m
Maximum transmit power of FBS	Pf,max	23 dBm
Minimal transmit power of MBS	Pf,min	− 40 dBm
Transmit power of MBS	$PtMBS$	43 dBm
PRBs assigned to high-rate user	Mu	3
PRBs assigned to low-rate user	Lu	1
Max transmit power of UEs	$Pmax$	23 dBm
Path loss compensation factor	α	1
Power to be contained in one PRB	Po	− 106 dBm
Path loss at 1 m	As	37 dBm
Path loss exponent	n	3
Thermal noise power	No	− 96.8 dBm
Wall penetration loss	Lw	12
No. of FBSs	Nf	2
No. of MBSs	Nm	1
Range modification step	$\Delta R+$	2
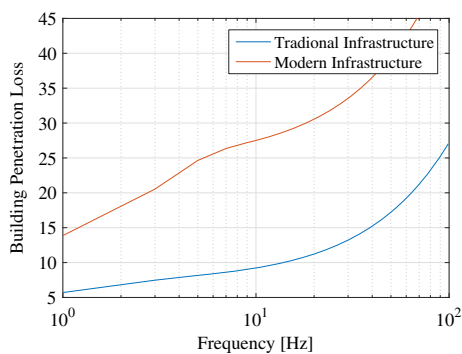
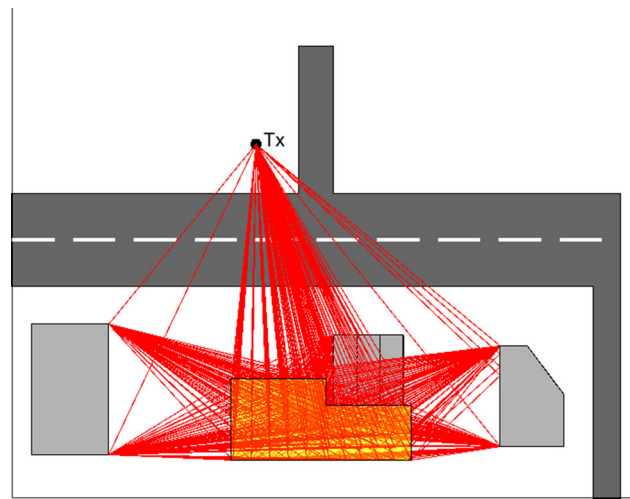**Fig. 10** Building penetration loss

Fig. 11 Ray tracing intelligent algorithm (2D) implementation in MAT-LAB

WIMAX, GSM, IEEE, LTE, 3GPP, 5G, etc. [21] Simulations were performed considering night scenarios, to avoid rough movements. A typical "macro-cell" is considered here for the state life building in Faisalabad, Punjab, Pakistan. The street width is 10 [m] and is separated by few trees with maximum height of 6 [m]. The building in the concerned area is mostly made of concrete, with different heights. For indoor path loss, we selected WINNER II A1 from [4], as it is accurate in recent models. WINNER II, in this paper is also compared with ITU-R for accuracy of results.

Figure 8 illustrates that we need three femto access points (FAPs) for the concerned scenario to cover. The winner II states that: [4]

$$PL_{LoS} = 46.8 + 18.7 * \log_{10}(d) + 20 * \log_{10}\left(\frac{fc}{5}\right) \quad (8)$$

$$PL_{NLoS} = 46.4 + 20 * \log_{10}(d) + 20 * \log_{10}\left(\frac{fc}{5}\right) + L_{w} \quad (9)$$

where fc represents the operating frequency of the base station, d is the separation between user terminal (UT) and base station (BS) and L_{w} is wall penetration loss which is $5(n_{w} - 1)$. On the other hand, ITU-R can be employed in variety of scenarios including offices, roadways, urban areas, rural areas and vehicular, etc. This makes ITU-R a semi-empirical propagation model. The path loss for LoS and NLoS between frequencies of 0.9 [GHz] to 6 [GHz] is given by ITU-R as [5]

$$Pl_{LoS} = 18 * \log_{10}(f_{c}) + N * \log_{10}(d) - 28 \quad (10)$$

$$Pl_{NLoS} = 20 * \log_{10}(fc) + N * \log_{10}(d) + L_{f(n_{w})} - 28 \quad (11)$$

where n_w is wall count and Lf represents wall penetration loss and is equal to 4 dB and $N = 28$ (power loss coefficient). The separation between FAPs and FUTs varies; therefore, the path loss is different for all FUTs. Table 2 illustrates the separation in [meters] between femto user terminal and access points. Path loss varies with distance. Longer distance increases the risk of higher path loss. According to [22], the first step for femto deployment is to calculate number of femtocells required on the basis of the area of an enterprise; the following formula is proposed:

$$\text{No. of femtos req} = \frac{\text{Area(ft}^2)}{\text{femto coverage area}} \qquad (12)$$

The above equation is formulated in consideration with interference. In our case, the area of one floor is approx. (41 [m] $\times$ 14 [m]) = 6179 [ft^2] and femto coverage area is 3380 [ft^2].

The intelligent femto deployment can be seen in Fig. 9. In this scenario, we just need 2 femto access points to fulfill the demand of 1 floor of our 15 floored enterprise building. It can be seen in Fig. 9 that the UT 7 is facing interference from both the FAPs. The second part of femtocell coverage planning is to identify the location for installation. Femtocell location plays a key role in a trade-off between interference, throughput and coverage. Inappropriate locations can lead to coverage holes. The femto coverage holes are due to the excessive distance from other FAP. Too close femtocells can cause excessive interference.

4 Ray Tracing or Deterministic Path Loss Modeling

The concept of ray tracing in RF was first introduced in Brute force algorithm and is used in this simulation. Brute force efficiently traces huge number of rays from transmitter to receiver in all directions. A reception sphere is required to detect the rays passing from receiver. Brute force is from the group of algorithms often called as rays launching, ray shooting and bouncing or pincushion method. On the other hand, the second concept of RT is ray tubes or beams. This reduces the complexity of the computations. Lastly, the third approach is related to entire scene surfaces [11]. RT (location-specific) models utilize theory of geometrical optics (GO) for reflections and transmissions on plan and smooth surfaces. Geometrical optics is basically rays approximations. In GO, it is assumed that the wavelength is smaller than the obstacles. The radio waves also behave same like light waves. That is why, the radio propagation can also be considered as rays propagation. Transmitter launches the rays, which interact with different objects and portions of the building using Fermat's principle. It states that "rays take the shortest path and time as they strike the boundaries, until and unless the

angles of incidence and the angles of reflection/transmission are equal." The approaches applied in RT models are of two types: (1) image theory [23] and (2) brute force method [24]. In brute force method, a transmitter transmits rays in all directions. Therefore, it is called as ray launching method. RT is achieved by a thorough examination of a rays hierarchy computing for breakdown of the rays at respective planar intersection. For every ray, we have to pattern each partition which is achieved by a 3D box. Computations are achieved when the ray crosses that 3D box. Brute force therefore requires a number of objects intersections test and large amount of ray data arrays. On the other hand, image method depends on the method of images, which links simulations with every obstacle and measures their effective transmission.

4.1 Ray Tracing For Macro-cell

A thorough geometrical sketch of the building is considered. The geometry of the building is in 3D. The nonplanar parts are broken down into chunks of planar surfaces to support the inputs into the model. The detailed steps involved in the model's framework are illustrated in Algorithm 1.

The floor plan is used in MATLAB; it gives the location of all the walls. All the columns in the plan are squares and represent a plane, i.e., counter, top, windows, ceilings, walls, and floors. The input to the model can be done from the left coordinates. Next step is to proceed counterclockwise. Electromagnetic properties and parameters are also put into the model for identification of the path of rays. Computation of reflections and transmissions coefficient can be done by using the electromagnetic properties of the walls. Electromagnetic properties include conductance, dielectric and permittivity. The receiver and transmitter databases consist of the coordinates and the location of receiver and transmitter, respectively, in the building coordinate's database. Multiple receiving points are made for the purpose of movement of UT (Table 3).

The description of the algorithm is as follows.

1. The first step is to generate a ray in both azimuth and elevation plane
2. While the ray is generated, the next step is to find the number of walls with which the ray is intersected.
3. Step three involves the reflection and diffraction of rays
4. After the reflection and diffraction, the ray is entered into the building. The ray then intersects with the obstacles in the building or inner wall, ceiling, etc.
5. The final step is to add all the path losses, i.e., through wall, in-building path loss, ceiling, reflected and diffracted ray.
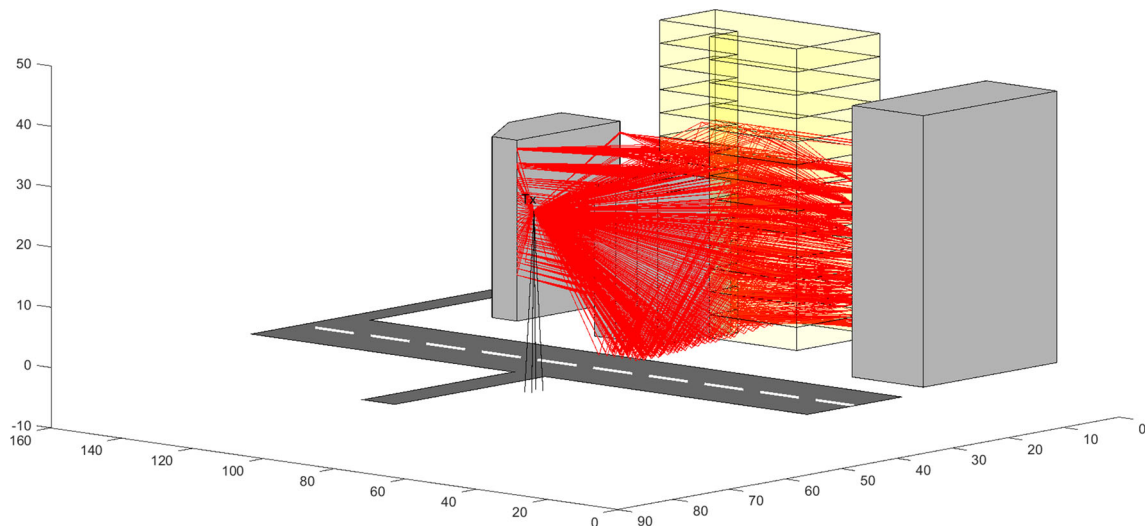
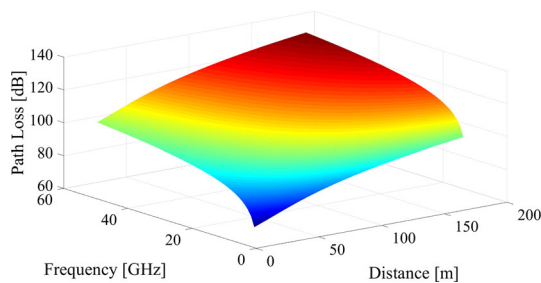**Fig. 12** Ray tracing intelligent algorithm (3D) implementation in MATLAB

Fig. 13 LoS: path loss as a function of distance and frequency "macro base station"

Equations (13) and (14) show the relation of reflection coefficient with material permittivity (ϵ_r) [19]

$$\Gamma_\perp = \frac{\sin(\beta) - \sqrt{\epsilon_r - \cos(\beta^2)}}{\sin(\beta) + \sqrt{\epsilon_r - \cos(\beta^2)}} \tag{13}$$

$$\Gamma_\parallel = \frac{-\epsilon_r \sin(\beta) + \sqrt{\epsilon_r - \cos(\beta^2)}}{\epsilon_r \sin(\beta) + \sqrt{\epsilon_r - \cos(\beta^2)}} \tag{14}$$

where β represents angles between the "incident rays" and the "reflected surfaces" and ϵ_r is the material permittivity of the reflected surface.

4.2 Ray Tracing for Femtocell

The algorithm followed for femtocell in indoor environment is same as described in Sect. 4.1.

5 Results and Discussion

This section explains the results of the simulations performed as discussed in Sect. 4.

5.1 Deterministic Versus Ray Tracing for Macro-cell

Figure 10 shows the building penetration loss. It can be seen that the building penetration loss (BPL) through new infrastructure is higher than BPL through the old infrastructure. This is due to the use of infrared reflective (IRR) glass. Figure 13 shows the path loss of macro base station to the receiver at different frequencies. The upper curves are for NLoS conditions as the propagation loss is greater than the LoS.
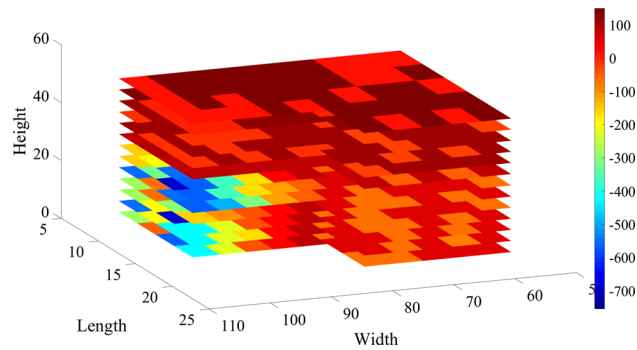
In Fig. 11, a smart ray tracing algorithm is implemented in MATLAB. Figure 11 shows the 2D ray tracing with outdoor transmitter TX and indoor receiver Rx in yellow building. The two-dimensional structure of the building is shown. Figure 12 is the 3D illustration of the algorithm and infrastructure. The transmitter is simulated outside of the building as in case of MBS. It can be seen that the rays are transmitted from the transmitted are reflected, refracted, deflected or diffracted when they find an obstacle in their path. Few of the RF rays reach the receiver directly (LoS).

Figure 12 shows the 3D ray tracing with transmitter height of 30 [m] and receiver on 1st floor. The red lines show different propagation paths between Tx and Rx with finite number of reflections, diffractions and direct path.

Figure 13 shows that the path loss for MBS is low for LoS as the transmitter and receiver face each other at same height, i.e., 30 [m]. The darkest yellow portion of the figure points out the loss is very high above 110 [db]. Figure 13 shows that the path loss for MBS is very high as the separation between transmitter and receiver 100 [m]. Again the
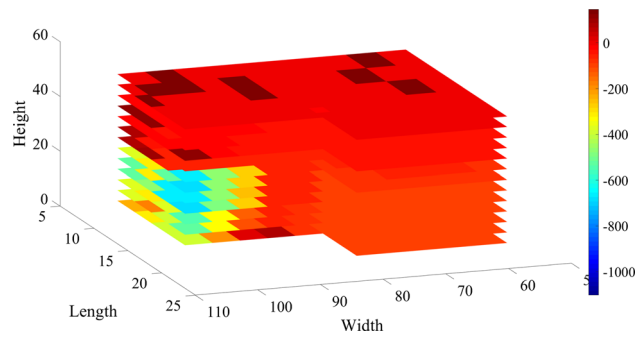
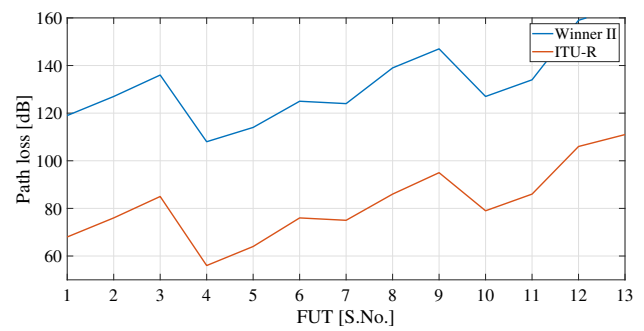Fig. 14 Path loss based on user location: Rx–Tx separation = 45 m

Fig. 16 Femto path loss for different FAPs)

Fig. 15 Path loss based on user location: Rx–Tx separation = 100 m
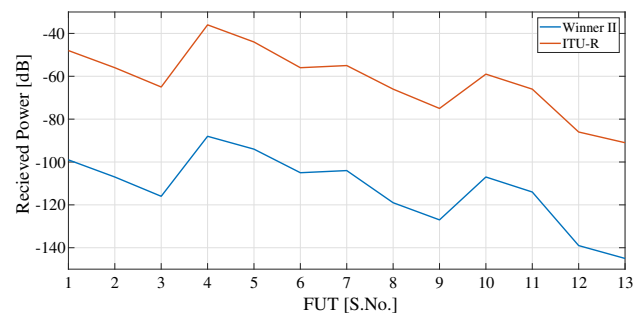

Fig. 17 Received power for each FUT

height of the Tx and Rx is same, i.e., 30 [m]. The darkest blue portion of the figure points out the loss is very high above 170 db. The reason behind this is the impact of a building standing infront of the concerned building. The LoS is lost and the path of rays coming to the receiver's building scatters, resulting in a dramatic increase in the path loss. Scale on the right side of both the figures (Figs. 14, 15) can be used to see the difference as we increase the separation, the intensity of received signal strength decreases, and the path loss increases. For simulating the ray tracing, building's surfaces are assumed smooth which acts as perfect reflector, in which incident and reflected angles are same. For receiver points are at different heights in the building, the incidence ray path penetrates through the ceilings. Therefore, ceiling penetration loss is added in the model. Generally, the ceilings are made up concrete. Therefore, concrete loss is used as ceiling loss.

5.2 Deterministic Versus Ray Tracing for Femtocell

In Fig. 16, (in the indoor environment), the femtocells are deployed on the basis of [22] and path loss for each FUT is calculated. Figure 16 shows that as we move away from FAP, the each FUT experiences different path loss due to the distance it has from FAP (Table 2 shows the distance of FAPs from individual FUTs). Considering power loss and

other losses such as wall penetration, WINNER II's average is lower by 5 [db] over ITU-R.

Figure 17 illustrates the received at each FUT. The received power shown tells that the power transmitted is decreased by approx. 20 [dB]. As a matter of fact, ITU-R has higher PL that is why the received power is slightly higher than the other model discussed model. The results discussed here illustrate that WINNER II is better than the ITU-R in all investigations because of the path loss coefficient.

Figure 18 shows the floor plan implementation in MATLAB. The scale is set such that each grid square represents 1 [m^2] The visibility of the walls and the edges of the walls can be found out by identifying the path of rays. Figure 19 shows the heatmap of the first-order reflection for indoor femto base station. The signal strength is visible as we move away from the FAP, the signal gets weaker. Reflection and diffraction can be produced from the first-order images which are visible from the walls. Figure 20 explains the second reflection of the femto access point. The result clearly illustrates that the second reflection is much stronger than the first one. Proposed RT model is using this type of visible to find out the path of rays. Figure 21 shows the line of sight reflection at vertical plane (azimuth plane).

The results demonstrated here express that

1. The path loss for O2I increases by approx. 100 [dB] when the distance is increased by 50 [m].
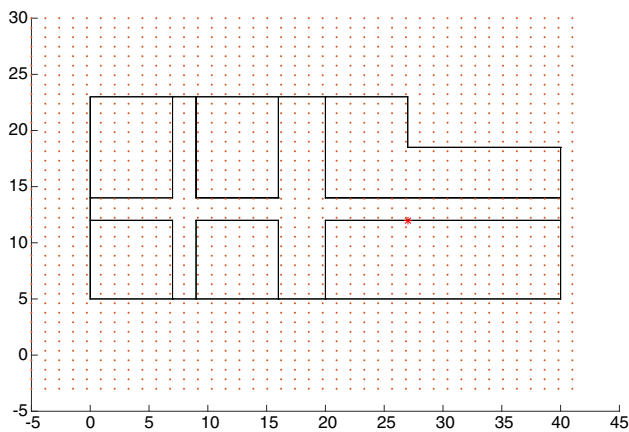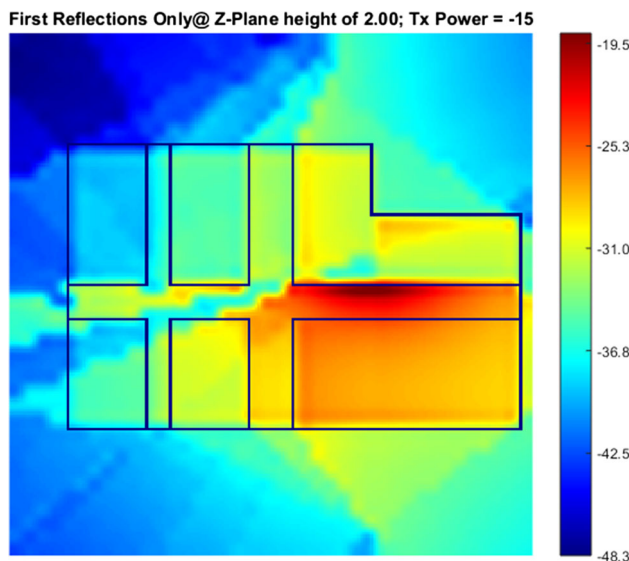
Fig. 18 Floor plan implementation in MATLAB
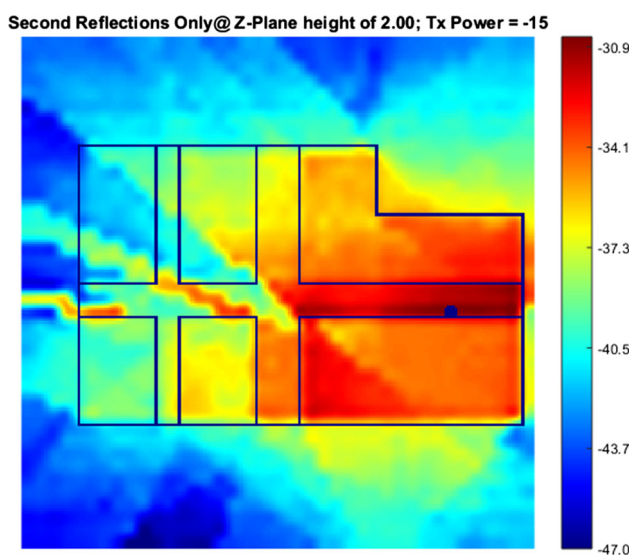

Fig. 19 1st reflection for FAP
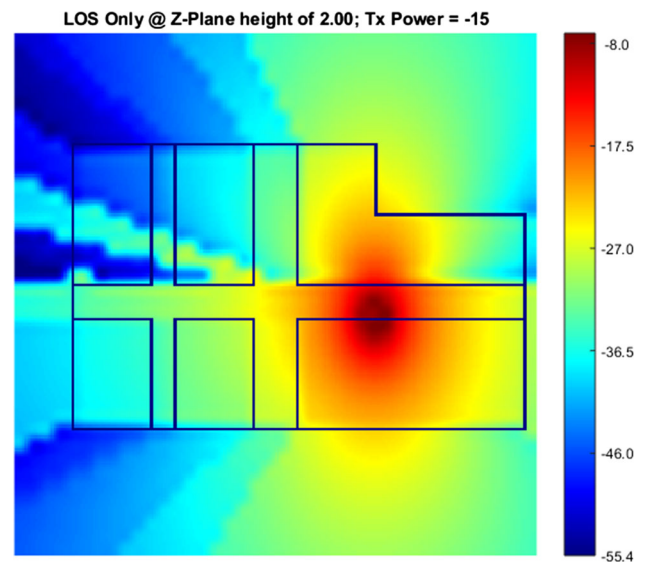

Fig. 20 2nd reflection for FAP

Fig. 21 LoS for FAP

2. If the windows of the building are of IRR glass kind, then a raise of 20 [dB] path loss is expected.
3. The direct path has a significant effect on radio propagation.
4. Femtocells can help in the reduction of path loss up to [50–60] dB.

6 Conclusion

Femtocells are smart and small base stations with low cost and high performance. An (smart 3D ray tracing) algorithm is proposed and is supported by the literature. Both approaches (ray tracing and deterministic) performed showed that femtocells are more reliable, self-configuring and economic base stations as compared to large macro-cells. This simulator can be further used for future development for algorithms related to 3D-MIMO RT by adding number of inputs and outputs antenna as transmitters and receivers, respectively, and changing the patterns of the antenna. Furthermore, this simulator can be used for higher bands by changes and updating some of the simulation parameters (e.g., operating frequency, antenna gain, received signal strength indicator, antenna loss, transmission loss, etc.). The path loss in macro-cells is affected by obstacles in the path of radio waves while femtocells are not exposed to such outdoor path losses. In this paper, brute force algorithm is modified for a unsymmetrical building with all the possible angles to make it accurate. The work done here also suggests that building material, distance and the frequency of radio wave propagation also constitute in building site-specific models.

Algorithm 1: Smart 3D Ray Tracing Algorithm

```
 1  ; for azi = 1 : 360 do
 2      for ele = 1 : 360 do
 3          Generate new-ray from Tx to Angle (azi, ele)
 4          ray = new-ray
 5          while no-intersection with outer-walls do
 6              for i = 1 : number of outer-walls do
 7                  if check-intersected (ray, outer-wall (i)) then
 8                      ray = diffraction (ray)
 9                      diffraction = diffraction + 1
10                  else
11                      ray = reflection (ray)
12                      reflection = reflection + 1
13                  end
14              end
15              if check-intersect (ray, boundary then
16                  if Rx b/w ray-ray then
17                      Draw ray
18                      for j = 1 : number of inner-walls do
19                          if check-intersect (ray, inner-wall(j))
                            then
20                              intersected-walls++
21                          end
22                      end
23                      PathLoss=PLb+PLtw+PLin+celling+
                        reflected+diffracted
24                  end
25              end
26          end
27      end
28  end
29 end
```

References

1. Ever, E.; Al-Turjman, F.; Zahmatkesh, H.; Riza, M.: Modelling green HetNets in dynamic ultra large-scale applications. Comput. Netw. Int. J. Comput. Telecommun. Netw. **128**, 78–93 (2017)

2. Kiran, J.; Nimavat, D.: Comparative analysis of path loss propagation models in radio communication. In: IJIRCCE, vol. 3, no. 2 (2015). http://www.ijircce.com/upload/2015/february/62_COMPARATIVE.pdf

3. 5G; Study on channel model for frequencies from 0.5 to 100 GHz (3GPP TR 38.901 version 15.0.0 Release 15)

4. Vuokko, N.; et al.: Deliverable D1.2: initial channel models based on measurements (2014). https://metis2020.com/wp-content/uploads/deliverables/METIS_D1.2_v1.pdf. Accessed 13 Jan 2020

5. International Telecommunication Union: Guidelines for evaluation of radio interface technologies for IMT-2020, Geneva, Switzerland Rec. ITU-R M.2135-1, December (2017)

6. Rappaport, T.S.; Heath, R.W.; Daniels, R.C.; Murdock, J.N.: Millimeter Wave Wireless Communications. Prentice Hall, Upper Saddle River (2015)

7. Pahlavan, K.; Levesque, A.H.: Wireless Information Networks. Wiley Series in Telecommunications and Signal Processing, 2nd edn, pp. 245–261. Wiley, Hoboken (2005). (John Proakis, Series Editor)

8. Seidel, S.Y.; Rappaport, T.S.: Site-specific propagation prediction for wireless in-building personal communication system design. IEEE Trans. Veh. Technol. **43**(4), 879–891 (1994)

9. Trueman, C. W.; Paknys, R.; Zhao, J.; Davis, D.; Segal, B.: Ray tracing algorithm for indoor propagation. In: ACES 16th Annual Review of Progress in Applied Computational Electromagnetics, Monterey, California, pp. 493-500, March 20–24 (2000)

10. Mishra, A.R.: Advanced Cellular Network Planning and Optimization 2G/2.5G/3G, Evolution to 4G. Wiley, New York (2007)

11. Bregar, K.; et al.: Evaluation of range-based indoor tracking algorithms by merging simulation and measurements. EURASIP J. Wirel. Commun. Netw. **2019**, 173 (2019)

12. Hossain, F.; et al.: A smart 3D RT method: indoor radio wave propagation modelling at 28 GHz. Symmetry **11**(4), 510 (2019)

13. Maccartney, G.R.; Rappaport, T.S.; Sun, S.; Deng, S.: Indoor office wideband millimeter-wave propagation measurements and channel models at 28 and 73 GHz for ultra-dense 5G wireless networks. IEEE Access **3**, 2388–2424 (2015)

14. MacCartney, G.R.; Rappaport, T.S.; Samimi, M.K.; Sun, S.: Millimeter-wave omnidirectional path loss data for small cell 5G channel modeling. IEEE Access **3**, 1573–1580 (2015)

15. Samimi, M.K.; Rappaport, T.S.; MacCartney, G.R.: Probabilistic omnidirectional path loss models for millimeter-wave outdoor communications. IEEE Wirel. Commun. Lett. **4**, 357–360 (2015)

16. Sulyman, A.I.; Nassar, A.T.; Samimi, M.K.; MacCartney, G.R.; Rappaport, T.S.; Alsanie, A.: Radio propagation path loss models for 5G cellular networks in the 28 GHz and 38 GHz millimeter-wave bands. IEEE Commun. Mag. **52**, 78–86 (2014)

17. Larsson, C.; Olsson, B.-E.; Medbo, J.: Angular resolved pathloss measurements in urban macrocell scenarios at 28 GHz. In: Proceedings of the 2016 IEEE 84th Vehicular Technology Conference (VTC-Fall), Montreal, QC, Canada, 18–21 September 2016, pp. 1–5

18. Huang, J.; Wang, C.-X.; Feng, R.; Sun, J.; Zhang, W.; Yang, Y.: Multi-frequency mmWave massive MIMO channel measurements and characterization for 5G wireless communication systems. IEEE J. Sel. Areas Commun. **35**, 1591–1605 (2017)

19. Sidhu, S.S.; Khosla, A.; Sharma, A.: Implementation of 3-D ray tracing propagation model for indoor wireless communication. Int. J. Electron. Eng. **4**(1), 43–47 (2012)

20. Samimi, M.; Rappaport, T.S.: 3-D millimeter-wave statistical channel model for 5G wireless system design. IEEE Trans. Microw. Theory Tech. **64**(7), 1–19 (2016). https://doi.org/10.1109/TMTT.2016.2574851

21. Anna, D.; et al.: Measurement-based coverage function for green femtocell networks. Comput. Netw. **83**, 45–58 (2015)

22. Enterprise Multi-Femtocell Deployment Guidelines. Incorporate qualcomm 2011. https://www.qualcomm.com/media/documents/files/qualcomm-research-enterprise-femtocell.pdf

23. Sheikh, M.U.; Hiltunen, K.; Lempiainen, J.: Enhanced outdoor to indoor propagation models and impact of different ray tracing approaches at higher frequencies. Adv. Sci. Technol. Eng. Syst. J. **3**(2), 58–68 (2018)

24. Majdi, S.; et al.: Validation of three-dimensional ray-tracing algorithm for indoor wireless propagations. ISRN Commun. Netw. Article ID 324758. http://downloads.hindawi.com/archive/2011/324758.pdf (2011)